F

NASA CR-121130
BMI-762-11

PREPARATION OF REFRACTORY CERMET STRUCTURES FOR LITHIUM COMPATIBILITY TESTING

by R. L. Heestand, R. A. Jones, T. R. Wright, and D. E. Kizer

BATTELLE MEMORIAL INSTITUTE

prepared for

NATIONAL AERONAUTICS AND SPACE ADMINISTRATION

NASA Lewis Research Center
Contract NAS 3-13465

(NASA-CR-121130) PREPARATION OF REFRACTORY CERMET STRUCTURES FOR LITHIUM COMPATIBILITY TESTING (Battelle Memorial Inst.) 48 p HC $4.50 CSCL 11D

N74-10543

Unclas
G3/18 21560

1. Report No.	2. Government Accession No.	3. Recipient's Catalog No.
NASA CR-121130		

4. Title and Subtitle	5. Report Date
PREPARATION OF REFRACTORY CERMET STRUCTURES FOR LITHIUM COMPATIBILITY TESTING	February 1973
	6. Performing Organization Code
7. Author(s)	8. Performing Organization Report No.
R. L. Heestand, R. A. Jones, T. R. Wright, and D. E. Kizer	BMI-762-11
	10. Work Unit No.
9. Performing Organization Name and Address	11. Contract or Grant No.
Battelle Memorial Institute Columbus, Ohio 43201	NAS 3-13465
	13. Type of Report and Period Covered
12. Sponsoring Agency Name and Address	Contractor Report
National Aeronautics and Space Administration Washington, D.C. 20546	14. Sponsoring Agency Code

15. Supplementary Notes

Work was done by Battelle Memorial Institute under subcontract to General Electric; Project Manager, John A. Milko, Materials and Structures Division, NASA Lewis Research Center, Cleveland, Ohio

16. Abstract

High-purity nitride and carbide cermets were synthesized for compatability testing in liquid lithium. A process was developed for the preparation of high-purity hafnium nitride powder, which was subsequently blended with tungsten powder or tantalum nitride and tungsten powders and fabricated into 3-in.-diameter billets by uniaxial hot pressing. Specimens were then cut from the billets for compatibility testing. Similar processing techniques were applied to produce hafnium carbide and zirconium carbide cermets for use in the testing program. All billets produced were characterized with respect to chemistry, structure, density, and strength properties.

17. Key Words (Suggested by Author(s))	18. Distribution Statement
Nitride and carbide cermets Fabrication Hot pressing	Unclassified - unlimited

19. Security Classif. (of this report)	20. Security Classif. (of this page)	21. No. of Pages	22. Price*
Unclassified	Unclassified	47	$3.00

* For sale by the National Technical Information Service, Springfield, Virginia 22151

PRECEDING PAGE BLANK NOT FILMED

TABLE OF CONTENTS

PRECEDING PAGE BLANK NOT FILMED

LIST OF FIGURES

PREPARATION OF REFRACTORY CERMET STRUCTURES FOR LITHIUM COMPATIBILITY TESTING

R. L. Heestand, R. A. Jones, T. R. Wright, and D. E. Kizer

SUMMARY

High-purity nitride and carbide cermets were synthesized for compatibility testing in liquid lithium. A process was developed for the preparation of high-purity hafnium nitride powder, which was subsequently blended with tungsten powder or tantalum nitride and tungsten powders and fabricated into 3-in.-diameter billets by uniaxial hot pressing. Specimens were then cut from the billets for compatibility testing. Similar processing techniques were applied to produce hafnium carbide and zirconium carbide cermets for use in the testing program. All billets produced were characterized with respect to chemistry, structure, density, and strength properties.

INTRODUCTION

Various nitride-metal and carbide-metal composites are currently under consideration as bearing materials in a lithium-cooled compact nuclear reactor. In order to assess the compatibility of these specified materials, it was necessary to prepare a series of high-purity specimens. Duplicate specimens were characterized with respect to density, microstructure, and strength.

The specific purpose of this program was to produce ten specimens, 1/4 in. by 1/4 in. by 2 in. long, of each of the following compositions for subsequent testing in lithium at GE-NSP:

(1) HfN-10 w/o W
(2) HfN-10 w/o TaN-10 w/o W
(3) HfC-10 w/o W
(4) HfC-10 w/o TaC-10 w/o W
(5) HfC-8 w/o Mo-2 w/o NbC
(6) ZrC-17 w/o W

The technique selected for fabrication of the desired specimens was uniaxial hot pressing.

Suitable hafnium nitride and hafnium carbide could not be obtained commercially; hence, they were synthesized as a part of the program. Attempts to synthesize hafnium nitride by methods reported in the literature

were unsuccessful; thus, procedures were developed in this study for the production of suitable quantities of high-purity, stoichiometric hafnium nitride. In addition, a procedure was developed for the synthesis of hafnium carbide of better quality than was available commercially.

Since the hafnium nitride-10 w/o tungsten composition was anticipated to be the most difficult material to densify and because time or funding were not available for the determination of optimum parameters for the densification of each composition, the parameters developed for this composition were to be used to fabricate the remaining specimens. The parameters developed consisted of pressing at 2100 C for 2 hr at a pressure of 10 000 psi. The conditions were found to be maximum for the available die materials.

All starting materials were characterized with respect to composition and impurity levels. Specimens of a specific composition were fabricated from a single lot of the refractory compound and metal binder phase.

Each lot of the finished corrosion test specimens was characterized with respect to impurity content, chemical composition, and spectrographic analysis. Physical properties determined were bulk density, dimensions, weight, and lattice parameters. Quantitative metallography was used to determine porosity and grain size distribution.

Mechanical properties were determined by conducting three-point bend tests for the determination of the modulus of rupture, and electron micrographs were taken of the resultant fracture surfaces.

EXPERIMENTAL PROGRAM

Procurement of Materials

The prime requirements in the procurement of materials were high purity, reasonable cost, and a satisfactory delivery date. In a precontract survey it was found that prices were high and powders of the desired purity were not generally available; however, no indication was given that problems would be encountered in receiving the desired material within a reasonable time.

Hafnium nitride powder available commercially was judged unacceptable on the basis of cost, purity, and oxygen content. Therefore, it was

decided to produce it at Battelle's Columbus Laboratories (BCL) from either hafnium powder or hafnium crystal bar. Crystal bar hafnium was selected on the basis of purity and cost.

No difficulty was indicated from commercial bids in obtaining zirconium carbide or tantalum carbide powders of an acceptable purity at a reasonable price. Zirconium carbide, tantalum carbide, and niobium carbide powders were therefore purchased at 99.9 percent purity as minus 325-mesh powder with a specification of 100 ppm oxygen or less. Based on the vendors' analyses, these materials were judged to be satisfactory; however, reanalysis indicated an extremely high oxygen content for the zirconium carbide.

Tungsten and molybdenum powders are not generally purchased to a low oxygen specification because of the relative ease of oxygen removal by high-temperature treatment in hydrogen or in vacuum. Two lots of tungsten powder were purchased. The first had a Fisher subsieve particle size of 1.29 microns. Later it was found that a more nearly continuous matrix could be obtained with a smaller particle size. Thus a second lot of tungsten powder with a particle size of 0.78 micron was purchased. The oxygen contents of both lots were unacceptable as received; however, the oxygen contents were reduced to an acceptable level by a hydrogen reduction treatment for 4 hr at 1100 C.

The initial oxygen content of the molybdenum powder purchased was too great and it was reduced by a heat treatment for 4 hr at 1100 C under a vacuum of 1×10^{-5} torr.

Tantalum metal was purchased to synthesize TaN instead of purchasing commercial TaN powder because of the unacceptable oxygen content of the commercial TaN powder. Spectrographic grade graphite powder was purchased for preparation of the carbides.

Chemical Analysis of Starting Materials

Because of the rigid requirements on oxygen content, all starting materials were reanalyzed for oxygen by either BCL or by an independent laboratory. All samples for gas analysis were prepared in the glove box and sealed in Ferro-vac iron cans with vacuum-melted tin lids. Cans and lids were included for standards in each set of analyses. Each canned specimen was also sealed in an argon-containing bottle for transfer to analysis.

Analysis for gaseous contaminants was originally conducted at BCL using the vacuum-fusion technique. Table 1 presents the analysis of starting materials submitted by the vendor and the duplicate analysis conducted at BCL for oxygen and carbon. No spectrographic reanalysis was

TABLE 1. ANALYSIS OF STARTING MATERIALS

Material	Source of Analysis	Impurity Level at Less Than Value Indicated[(a)], ppm												
		O[(b)]	Si	Fe	Mg	Mn	Al	Mo	Co	Ni	Cr	Ca	C (w/o)	C_{free}
Hf Lot A	Vendor	50	40	50	10	10	30	5	20	10	10	-	-	-
	BCL		10	10	5	-	10	10	5	10	-	-	-	-
Hf Lot B	Vendor	50	-	50	-	-	30	5	20	10	10	-	-	-
	BCL													
Tungsten	Vendor	-	6	11	4	1	2	10	1	22	10	1	-	-
As received	BCL	1550												
reduced	BCL	26												
Molybdenum	Vendor	-	72	40	10	10	20	-	10	22	10	10	-	-
As received	BCL	420												
reduced	BCL	100												
Tantalum	Vendor	40	58	27	-	-	20	10	25	10	10	-	30	-
	BCL	50												
ZrC	Vendor	50	20	50	50	10	10	-	-	-	-	-	11.64	200
	BCL	2800											10.90	-
TaC	Vendor	80	2	5	-	-	-	-	-	-	-	-	6.31	200
	BCL	1000											6.10	-
NbC	Vendor	260	10	30	-	-	-	-	-	-	-	-	11.74	3900
	BCL	260											11.20	-

(a) - denotes below level of detection.
(b) Battelle value analyzed by inert-gas fusion.
(c) Analyzed for each batch, see Table 2.

conducted except in the case of the largest lot of crystal bar hafnium, which represented over 90 percent of the material utilized. Oxygen analysis for each batch of hafnium prepared for hydriding is presented separately in Table 2 since it was expected that oxygen content would vary throughout the length of the crystal bar. In the case of the refractory-metal powder used as a matrix, oxygen values after hydrogen or vacuum reduction are also reported for comparison.

Excessive oxygen contamination was found in both the zirconium and tantalum carbides. These analyses were conducted by an independent laboratory by inert-gas fusion and were not received until after fabrication of the zirconium carbide specimens was initiated.

Table 2 lists the oxygen and hydrogen analyses conducted throughout processing of the hafnium and tantalum powders to the nitrides. As discussed previously, analysis for oxygen content was originally conducted at BCL using the vacuum-fusion technique. In initial hot-pressing experiments, however, errors in analysis were indicated when a reduction in oxygen content occurred when comparing the hafnium nitride powder analysis to the analysis of hot-pressed hafnium nitride for Batches Hf-A and Hf-E. Since this reduction in oxygen content is not thermodynamically feasible, the oxygen content of the samples was checked by an independent laboratory utilizing the inert-gas-fusion process. Table 2 presents the original analysis of the powder batches by vacuum fusion and reanalysis of the nitride powders by inert-gas-fusion. Since the inert-gas-fusion technique appeared to be more consistent and technically was judged more reliable, this technique was utilized throughout the remainder of the program. Further hydrogen analyses were not conducted on the hafnium nitride powders because of the low hydrogen content of the dehydrided powders and the long exposure to high temperature in vacuum during subsequent fabrication. Since a low oxygen content was indicated by vacuum-fusion analysis, Batches Hf-B, Hf-D, Hf-E, and Hf-F were blended for use in fabricating the HfN specimens.

Due to the limited time available for preparation of the carbides and the high purity obtained on the nitride powders it was decided that an analysis of the powder prior to carbonization would not be taken. Further, it was concluded that the hydrided powder could be used directly to blend with the spectrographic-grade graphite. This modification eliminated the several hours of exposure at elevated temperature required to dehydride the hafnium as well as the crushing operation which would be required if the dehydriding operation was performed. These modifications would be expected to produce material with an extremely low oxygen content.

Synthesis of High-Purity Materials

Hafnium Nitride

Attempts to procure high-purity hafnium nitride powder from commercial sources were unsuccessful; therefore, crystal bar hafnium stock was procured in order to conduct the nitriding operation at BCL. The zirconium content of the crystal bar was anticipated to be as high as 3.5 w/o. However, the chemical

TABLE 2. ANALYSIS OF MATERIALS SYNTHESIZED FOR NITRIDES[a]

		Vacuum-Fusion Results, ppm				Inert-Gas-Fusion Analysis, ppm	
Material Batch	Element	Crystal Bar	Metal Powder	Nitride Powder	Hot-Pressed Nitride	Nitride Powder	Hot-Pressed Nitride
Hf-A, <100 g	O	212	525	1225	260	-	320
	H	8	32	-	-	-	-
Hf-B	O	155	180	475	-	108	237
	H	4	3	-	-	-	-
Hf-C, <100 g	O	255	660	1100	-	-	130
	H	20	20	-	-	-	-
Hf-D	O	710	715	1900	-	100	-
	H	110	75	-	-	-	-
Hf-E	O	212	235	2650	300	170	-
	H	8	25	-	-	-	-
Hf-F	O	155	-	-	-	75	-
	H	4	-	-	-	-	-
Tantalum	O	50	-	-	-	79	-
	H	2	-	-	-	-	-

(a) - denotes not analyzed.

similarity of hafnium and zirconium and hafnium nitride and zirconium nitride indicated there would be no significant difference in performance of the material.

The process selected to synthesize hafnium nitride consisted of reducing the crystal bar hafnium to the powder by hydriding,[1] with conversion to the nitride utilizing procedures previously reported in the literature.[2]

Initially, the crystal bar hafnium was cleaned by etching in a solution of 45 v/o nitric acid-5 v/o hydrofluoric acid-50 v/o water, followed by rinsing in water and ultrasonic cleaning in absolute ethyl alcohol. It was noted that this procedure gave a slight discoloration to the surface of the crystal bar, indicating an anodic film; thereafter, cleaning was limited to ultrasonic degreasing in absolute ethyl alcohol. At this point the cleaned crystal bar was introduced into a vacuum-purged, inert-atmosphere glove-box furnace apparatus.

The glove box was purged by evacuating to a minimum pressure of 1×10^{-5} torr and backfilling with purified argon. Both the moisture level and oxygen content of the glove box were monitored continuously, and the atmosphere was circulated through a purifier when water-vapor contamination increased to an equivalent dew point of -65 F. When the glove box was not in use, all materials were sealed in containers and the atmosphere was recirculated through the purifier continuously. All materials entering or removed from the glove box pass through an isolated, independently evacuated and purged interlock.

The material was placed in tungsten crucibles which were placed in a tungsten mesh furnace attached to the glove box. Batches were 1550 to 2000 g. The door between the furnace and glove box was sealed and the furnace chamber was evacuated to 1×10^{-5} torr. The material was heated to 700 C while maintaining a minimum vacuum of 1×10^{-5} torr. At 700 C, 1 atm of hydrogen was introduced and the temperature was increased to 860 C to initiate the hydriding reaction. Hydrogen utilized throughout the program was a 99.95 percent prepurified grade having a maximum equivalent dew point of -75 F and an oxygen content of less than 25 ppm. After initiation of the hydriding reaction, the temperature was reduced to 750 C. Time to complete hydriding varied with the amount of hafnium present; however, it was found that 15 hr at temperature was sufficient for complete hydriding of the larger batches of material.

Considerable swelling and cracking of the hafnium crystal bar occurred during hydriding; however, the starting pieces were intact after hydriding. Crushing of the material was conducted in the glove box in a hardened steel mortar and pestle to a particle size of minus 150 mesh. Sufficient material was processed for all specimens containing hafnium nitride and hafnium carbide.

Dehydriding of the minus 150-mesh powder was conducted at 860 C under vacuum. Completion of the reaction was indicated at a continuous pressure of 1×10^{-4} torr. To minimize time at temperature, dehydriding was accomplished on batches of 750 g. This size batch required approximately 2.5 hr for dehydriding. During this treatment slight sintering occurred; however, the powder mass was easily crushed to minus 150 mesh size. Sufficient material was processed by this method to produce all specimens containing hafnium nitride.

Initial attempts to synthesize small batches (<100 g) of hafnium nitride according to the literature[2] were unsuccessful. These attempts consisted of heating to 1500 C under 1 atm of nitrogen for 5 hr. Two distinct layered phases were identified on the hafnium powder particles. These phases were identified as HfN and Hf_2N. It was also found that considerable sintering of hafnium powder occurred in the center of the charge. Several experimental nitriding cycles were run while increasing the temperature and/or time at temperature; however, sintering of hafnium in the center of the charge persisted. To alleviate this problem and to obtain homogeneous material a two-step nitriding process was developed. In the first step the hafnium powder was heated to 800 C in nitrogen for 2 hr to form a nitride layer to inhibit sintering. The temperature was then raised to 1800 C in nitrogen for a period of 15 hr. After this treatment the material was crushed to minus 150 mesh and renitrided at 1800 C for an additional 15 hr. Material given the two-step treatment described resulted in homogeneous, single-phase hafnium nitride. Lattice parameters on a representative sample were determined as $A_o = 4.526 \pm 0.001$ with no other phases present. Approximately 6 kg of high-purity hafnium nitride was prepared for the corrosion test specimens. All nitrogen used in the preparation of nitrides was a 99.997 percent prepurified grade having a maximum equivalent dew point of -85 F and an oxygen content less than 35 ppm.

Hafnium Carbide

Hafnium carbide powder was synthesized by reacting hafnium hydride with spectrographic-grade graphite powder at elevated temperature in an ATJ graphite crucible which had been previously outgassed at 2000 C in a vacuum of 1×10^{-5} torr. Hafnium hydride was utilized instead of hafnium metal powder because the high reactivity of the hydride relative to the metal powder allowed a shorter reaction time.

On an initial run, swelling of the hafnium-carbon powder mass was sufficient to rupture the graphite crucible prior to completion of the reaction. In the preparation of subsequent batches the graphite crucible was lined with carbon felt and an inner layer of Grafoil to allow for swelling of the powder mass.

The conditions used for preparation of the hafnium carbide consisted of reacting the hafnium hydride-graphite powder blend in hydrogen for 4 hr at 1800 C followed by crushing to minus 150-mesh powder. The powder was then placed in a tungsten crucible and heated in a vacuum at a maximum pressure of 1×10^{-5} torr at 2300 C for 4 hr. The powder was single phase and had a lattice parameter of $A_o = 4.642 \pm 0.001$. Approximately 8 kg of material was synthesized for the corrosion test specimens.

Tantalum Nitride

Essentially the same process as used for hafnium nitride was applied for the preparation of tantalum nitride powder. Tantalum was received as rod which

was ultrasonically degreased in absolute ethyl alcohol. Hydriding was conducted in the glove-box furnace in an outgassed tungsten crucible by heating the material to 800 C under 1 atm of hydrogen for 10 min. The temperature was then dropped to 620 C and held for 15 hr. The resultant material was crushed to minus 150-mesh powder. Dehydriding was conducted by heating the tantalum hydride at 800 C under vacuum until a pressure of 1×10^{-5} torr was reached. The tantalum powder exhibited slight sintering but was readily crushed to minus 150-mesh powder.

Nitriding of this powder was conducted by heating to 1800 C for 15 hr under 1 atm of nitrogen. This material was crushed to minus 200 mesh and again heated to 1800 C for 15 hr under 1 atm of nitrogen. At this point X-ray analysis indicated the presence of Ta_2N; therefore, the material was subjected to a third nitriding cycle of 15 hr at 2000 C under 1 atm of nitrogen. This material was then crushed to minus 200-mesh powder. At this point an X-ray analysis indicated the major phase to be TaN with traces of Ta_2N present. Lattice parameters were determined as $A_o = 5.186\pm0.005$ and $C_o = 2.900\pm0.005$.

At this point no additional degree of conversion was anticipated by further high-temperature treatment; therefore, the material was used as an additive.

Blending Studies

It was desired to obtain a continuous metal matrix in all specimens in order to increase resistance to mechanical shock. Three techniques examined for blending were: (1) simple blending, (2) wax coating, and (3) ball milling.

Simple blending of the powders produced a structure in which the tungsten powder was agglomerated in large particles dispersed throughout the structure and was considered unsatisfactory. Wax coating of the HfN powder followed by coating with tungsten powder produced a structure in which a thin, discontinuous coating of tungsten occurred on each particle; however, agglomeration of large tungsten particles was also noted. This agglomeration is thought to be due to adhesion of tungsten to wax particles produced during screening of the wax-coated HfN. Figure 1 shows the dispersion of tungsten (gray phase) obtained by the wax coating technique. This sample was hot pressed for 4 hr at 1800 C with a load of 15 ksi. The porosity (black phase) in the structure is a result of the low temperature employed in this early pressing.

Ball milling of the tungsten and HfN powders for 15 hr under an argon atmosphere produces a fine-grained structure in which the tungsten is evenly dispersed throughout the sample as discontinuous particles along the grain boundaries. Figure 2 shows this type of structure. Densification of this sample was accomplished by hot pressing for 2 hr at 2200 C under a load of 15 ksi. It will be noted that the higher temperature used in hot pressing was very effective in reducing the porosity. None of the techniques employed for the addition of tungsten were successful in producing a continuous metal

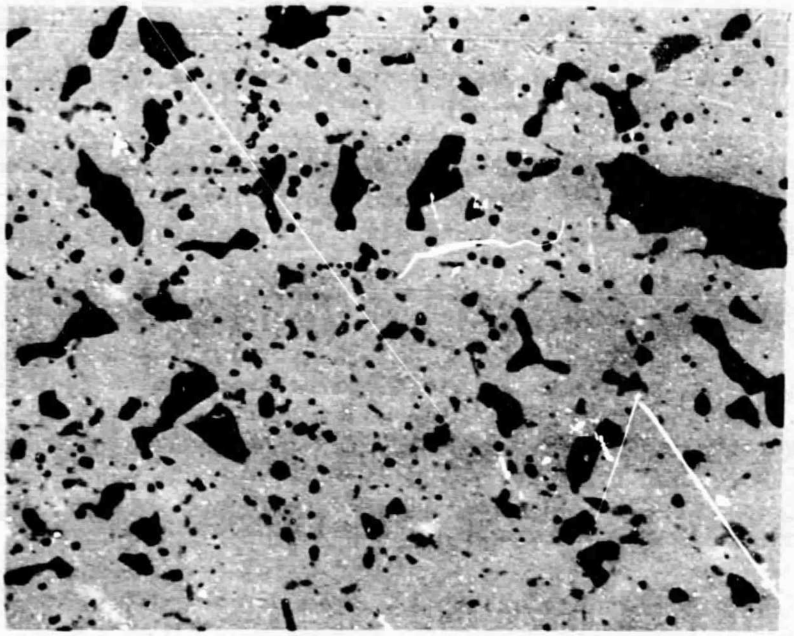

750X OF071

FIGURE 1. HfN-10 w/o TUNGSTEN HOT PRESSED AT 1800 C FOR 4 HR WITH A LOAD OF 15 KSI

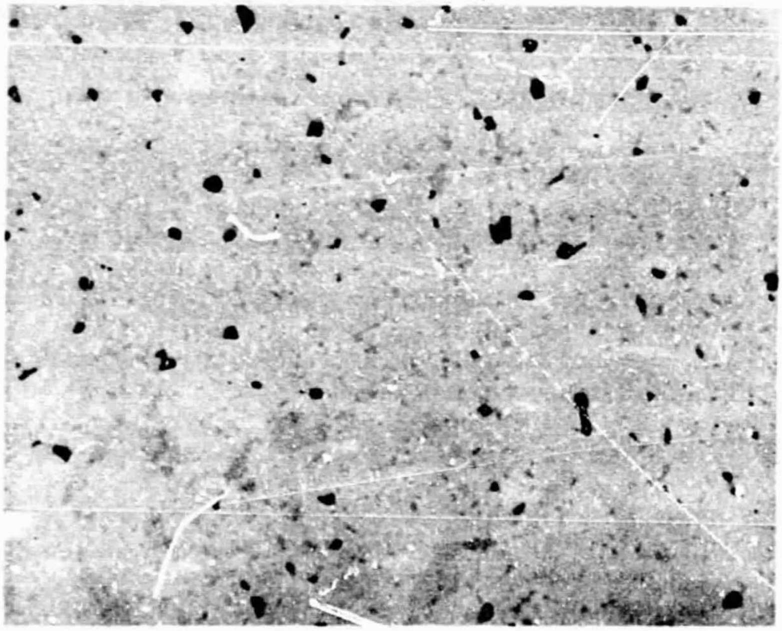

750X OF258

FIGURE 2. HfN-10 w/o TUNGSTEN BALL MILLED AND HOT PRESSED AT 2200 C FOR 2 HR WITH A LOAD OF 15 KSI

matrix due to the low volume of powder. Therefore, if a continuous refractory-metal matrix is found to be a requirement in future studies, it is suggested that the tungsten content be increased to 20 v/o or that alternative techniques, such as chemical vapor deposition of the refractory metal onto the powder particles, be considered. After review of the structures obtained with GE-NSP personnel, the ball milling approach was selected to produce the required test samples.

Hot Pressing

Preliminary Studies

Since originally it was anticipated that the greatest difficulty would be experienced in obtaining interparticle bonding in compositions containing hafnium nitride, hot-pressing experiments were conducted primarily on the HfN-10 w/o W composition. The parameters determined for densification of the hafnium nitride-tungsten were then to be utilized as maximum parameters for the fabrication of the remaining compositions. Initial experiments to determine densification parameters were conducted in small vacuum-inert atmosphere hot presses. At a temperature of 1800 C under pressing pressures of 15 ksi, structures such as that previously shown in Figure 1 were obtained; these structures contained a considerable amount of porosity. A large amount of residual porosity was also present when hot pressing was conducted at both 1900 C and 2000 C under 15 ksi. However, at 2200 C with a pressure of 15 ksi, structures such as that exhibited in Figure 2 were obtained; these were considered to be of satisfactory density. At this temperature and pressure, however, considerable plastic deformation of the graphite dies and punches occurred, which indicated that difficulties would be encountered with rupture of the graphite dies when pressing the large specimens required. For this reason and to determine the behavior of the dies and materials under full-scale conditions, a 3-in.-diameter by 1/2-in.-thick specimen of HfN-10 w/o tungsten was hot pressed at 2100 C under a load of 19 ksi for 2 hr utilizing a large hot press. A structure similar to that shown in Figure 2 was obtained which was also judged to have sufficient density. On this basis, hot pressing of the specimens required for corrosion testing was initiated.

Hot Pressing of Billets

Billets hot pressed for the corrosion and material characterization specimens were prepared in pairs from single batches of powder blends of the desired composition. Each batch was blended for 15 hr by ball milling in argon prior to hot pressing. Dies utilized consisted of a reusable ATJ graphite die body with sacrificial ATJ sleeve inserts and reusable AXF graphite punches. Sacrificial ATJ disks were placed between the composition to be pressed and the AXF punches in order to eliminate bonding or damage to the AXF punches. The die cavity was lined with one layer of Grafoil followed by a 0.001-in. layer of tungsten to minimize contamination of the billet material.

All graphite utilized in the punches and corollary furnace insulation was outgassed at 2100 C under a vacuum of 1×10^{-5} torr prior to the hot pressing of billets.

A weighed amount of powder was loaded into the die in the glove box to yield a billet approximately 0.400 in. thick. The loaded die body was then transferred into the hot press and evacuated to less than 1×10^{-5} torr prior to the application of heat. Heatup time to 2100 C was approximately 3 hr in each case. Pressure was applied to the powder after a 1-hr hold at temperature. It was attempted to hold all billets a minimum of 2 hr at temperature and pressure. Ram movement was monitored during each run to establish an end point to densification. It was judged that billet densification was complete when a ram movement of 0.004 in. per hr was measured; this was representative of the creep rate of the graphite punches under the pressing conditions.

Hot-pressing parameters for each billet are listed in Table 3. No difficulties occurred in the pressing of compositions containing hafnium nitride as the major constituent. In the pressing of hafnium carbide, however, considerable difficulty was encountered in achieving densification. Although a pressing rate of 0.004 in. per hr was attained for Billet 5, total punch travel indicated that the required density had not been achieved. In past experience, excessive punch and die creep usually precede die failure; therefore, pressing was terminated. Upon removal of Billet 5 from the die it was necessary to break the graphite die body because creep had upset the punch ends and the die body was bulging. Measurement of the hot end of the AXF punches indicated an increase in diameter from 2.90 to 3.20 in. In pressing Billet 6, temperature was increased to 2200 C to enhance densification and pressure was held for 3 hr; however, again, insufficient total ram travel indicated low density. At this point these billets were held for repressing at the end of the program since it was anticipated that die sets would be lost as a result of failure during pressing at the higher temperatures and pressures.

On repressing Billet 6 at the end of the program, it was attempted to achieve a higher density by heating to 2100 C and applying a pressure of 10 ksi for 2 hr followed by increasing the pressure in 1-ksi increments with 10-min holds until 15 ksi was reached. The maximum pressure was held for 4 min before the die failed catastrophically. At the failure, partial loss of vacuum also occurred; however, a vacuum value of 3×10^{-5} torr was attained in approximately 12 min.

Because of the low densities obtained when pressing the HfC-10 w/o W specimens, temperature was raised to 2200 C for pressing the remaining hafnium carbide specimens.

The bulk density measured for Billet 9 indicated low density; therefore, the pressure was increased to 12 ksi for pressing Billet 10. A die failure occurred after 30 min at pressure, and a bulk density comparable to that of Billet 9 was measured.

Difficulties were also encountered in pressing Billets 11 and 12, ZrC-17 w/o tungsten, as a result of the high solubility of tungsten in zirconium carbide. In each case sticking occurred with the punch and die inserts due to solution of the tungsten foil. Considerable cracking of the billet surface was also observed upon removal of the adhering graphite.

TABLE 3. PRESSING CONDITIONS FOR CORROSION TEST SPECIMENS

Billet	Material	Temperature, C	Pressure, ksi	Time, hr:min	Comments
1	HfN-10 w/o W-A	2100	10	2:30	Final ram movement - 0.004 in./hr
2	HfN-10 w/o W-B	2100	10	2:00	Final ram movement - 0.004 in./hr
3	HfN-10 w/o TaN-10 w/o W-A	2100	10	2:40	Final ram movement - 0.004 in./hr
4	HfN-10 w/o TaN-10 w/o W-B	2100	10	2:30	Final ram movement - 0.004 in./hr
5	HfC-10 w/o W-A	2100	10	2:30	Final ram movement - 0.004 in./hr; insufficient densification
5A	HfC-10 w/o W-A	2100	10	1:00	Repress Billet 5; ram aborted due to leak in lower ram
6	HfC-10 w/o W-B	2200	10	3:00	Final ram movement - 0.004 in./hr; insufficient densification
6A	HfC-10 w/o W-B	2100	10 15	2:00 0:04	Increased pressure in 1-ksi increments to 15 ksi; die failed
7	HfC-10 w/o TaC-10 w/o W-A	2200	10	3:30	Final ram movement - 0.004 in./hr
8	HfC-10 w/o TaC-10 w/o W-B	2200	10	3:30	Final ram movement - 0.004 in./hr
9	HfC-8 w/o Mo-2 w/o NbC-A	2200	10	3:00	Final ram movement - 0.004 in./hr
10	HfC-8 w/o Mo-2 w/o NbC-B	2200	12	0:30	Die failed
11	ZrC-17 w/o W-A	2100	10	3:30	Final ram movement - 0.004 in./hr
12	ZrC-17 w/o W-B	2100	10	4:00	Final ram movement - 0.004 in./hr

In the pressing of Billet 11 it was also observed that a loss in vacuum and considerable offgassing occurred at a temperature of approximately 2050 C. Analysis of the oxygen content of the starting powder by inert-gas fusion had not been received at the time of pressing; however, upon analysis the powder was found to contain 2800 ppm oxygen. It was apparent at this point that the offgassing could be attributed to the carbothermic reduction of the oxide present. In order to reduce the oxygen content of the remaining zirconium carbide powder before further hot pressing, the material was heated at 2100 C until a vacuum of 1 x 10^{-5} torr could be maintained. Subsequent analysis of Billet 12, hot pressed from material treated in this way, indicated a reduction in oxygen content.

Specimen Grinding

Cutting 1/4 by 1/4 by 2-in. specimens from the 3-in.-diameter billets was accomplished by grinding and slitting with diamond wheels. The procedure used consisted of grinding faces of the billet flat and parallel using 180- or 200-grit, 1/2-in.-wide wheels. Billets were then cut into approximately 0.260-in.-wide specimens by slitting one-half the thickness of the specimen from one side followed by slitting through the specimen from the opposite side. This procedure was utilized to prevent chipping of specimen edges which occurs when slitting from one side. Resultant specimens were then surface ground to the required 0.250 by 0.250-in. dimensions and cut to the 2.000-in. length.

Specimens 0.125 by 0.125 by 1.00 in. were cut from material adjacent to the corrosion test specimens for modulus of rupture testing.

Dimensions, bulk density, and average surface roughness for each set of specimens are reported in Tables 4 through 9.

Characterization of Billets

Analysis for the major constituents and oxygen contents for representatives samples from each hot-pressed billet are listed in Table 10. Compositions of additives agree with the chemical analysis with the exception of the tungsten content in the zirconium carbide samples. Losses in this instance may have occurred through vaporization of WO_3 formed from residual oxygen in the zirconium carbide; however, additional experiments and a study of the analytical accuracy would be required to determine the exact cause of the loss.

Nitrogen levels in hafnium nitride are low in comparison to values given in the literature for the measured lattice parameters. However determination of nitrogen in hafnium nitride is not a routine analysis, and several duplicate analyses should be conducted in order to verify the values.

All oxygen analyses were conducted by the vacuum-fusion technique, and are judged to be accurate. Of particular interest is the reduction in oxygen content of the zirconium carbide hot-pressed specimen after vacuum treatment of the zirconium carbide powder.

TABLE 4. MEASUREMENTS OF HfN-10 w/o TUNGSTEN SPECIMENS (RMS 38-44)

Specimen	Length, in.	Width, in.	Thickness, in.	Weight, g	Density, g per cm^3
A-1	1.9996	0.2514	0.2513	27.6307	13.37
A-2	1.9994	0.2514	0.2504	27.6611	13.42
A-3	2.0000	0.2514	0.2503	27.6168	13.39
A-4	1.9994	0.2513	0.2503	27.4140	13.31
A-5	1.9995	0.2511	0.2503	27.6528	13.44
B-1	1.9994	0.2509	0.2499	27.5172	13.42
B-2	1.9994	0.2512	0.2475	27.3536	13.45
B-3	1.9990	0.2513	0.2497	27.5051	13.40
B-4	1.9997	0.2514	0.2487	27.4933	13.43
B-5	1.9993	0.2513	0.2503	27.5835	13.39

TABLE 5. MEASUREMENTS OF HfN-10 w/o TaN-10 w/o TUNGSTEN SPECIMENS (RMS 27-32)

Specimen	Length, in.	Width, in.	Thickness, in.	Weight, g	Density, g per cm^3
A-1	1.999	0.250	0.250	28.461	13.85
A-2	2.000	0.250	0.250	28.389	13.86
A-3	2.000	0.250	0.250	28.414	13.87
A-4	2.000	0.250	0.250	28.327	13.83
A-5	1.999	0.250	0.250	28.458	13.86
B-1	2.000	0.250	0.249	28.328	13.85
B-2	2.000	0.250	0.249	28.351	13.84
B-3	2.000	0.250	0.249	28.373	13.85
B-4	2.000	0.250	0.249	28.331	13.85
B-5	2.000	0.250	0.249	28.285	13.85

TABLE 6. MEASUREMENTS OF HfC-10 w/o TUNGSTEN SPECIMENS (RMS 82-87)

Specimen[a]	Length, in.	Width, in.	Thickness, in.	Weight, g	Density, g per cm^3
A-1	2.001	0.244	0.249	20.263	10.063
A-2[b]	2.001	0.250	0.250	20.808	10.681
A-3	2.001	0.243	0.250	20.354	10.157
A-4	2.001	0.250	0.250	20.804	10.663
A-5	2.001	0.250	0.250	20.766	10.631
B-1	1.994	0.250	0.250	20.911	10.772
B-2	2.001	0.250	0.250	20.913	10.740
B-3	2.001	0.250	0.250	20.9712	10.754
B-4	2.001	0.250	0.250	20.993	10.768
B-5	2.001	0.250	0.250	21.014	10.796

(a) All specimens contain flaws.

(b) Broken.

TABLE 7. MEASUREMENTS OF HfC-10 w/o TaC-10 w/o TUNGSTEN SPECIMENS (RMS 48-52)

Specimen	Length, in.	Width, in.	Thickness, in.	Weight, g	Density, g per cm^3
A-1	2.000	0.248	0.250	23.876	11.76
A-2	2.000	0.249	0.249	24.225	11.93
A-3	2.000	0.249	0.250	24.245	11.94
A-4	2.001	0.249	0.250	24.136	11.88
A-5	2.000	0.249	0.250	24.160	11.90
B-1	2.000	0.250	0.250	24.263	11.85
B-2	2.001	0.248	0.250	24.267	11.95
B-3	2.000	0.250	0.250	24.252	11.84
B-4	2.002	0.250	0.250	24.217	11.83
B-5	2.001	0.250	0.250	24.253	11.84

TABLE 8. MEASUREMENTS OF HfC-8 w/o MOLYBDENUM-2 w/o NbC SPECIMENS (RMS 44-50)

Specimen	Length, in.	Width, in.	Thickness, in.	Weight, g	Density, g per cm^3
A-1	2.001	0.250	0.251	22.554	11.02
A-2	2.000	0.250	0.251	22.600	11.04
A-3	2.001	0.250	0.251	22.834	11.12
A-4	2.001	0.250	0.250	22.931	11.20
A-5	2.000	0.250	0.250	22.709	11.10
B-1	2.000	0.250	0.251	22.912	11.19
B-2	2.000	0.250	0.251	22.929	11.19
B-3	2.001	0.250	0.251	22.677	11.07
B-4	2.001	0.250	0.251	23.065	11.26
B-5	2.000	0.250	0.251	22.746	11.11

TABLE 9. MEASUREMENTS OF ZrC-17 w/o TUNGSTEN SPECIMENS (RMS 10-15)

Specimen	Length, in.	Width, in.	Thickness, in.	Weight, g	Density, g per cm^3
A-1	2.001	0.249	0.250	14.287	7.31
A-2	2.001	0.249	0.250	14.254	7.29
A-3	2.001	0.249	0.250	14.419	7.37
A-4	2.001	0.249	0.250	14.397	7.36
A-5	2.001	0.250	0.250	14.277	7.29
B-1	2.001	0.250	0.250	14.423	7.38
B-2	2.001	0.250	0.250	14.451	7.39
B-3	2.001	0.250	0.250	14.395	7.36
B-4	2.001	0.250	0.251	14.324	7.34
B-5	2.001	0.249	0.250	14.324	7.32

TABLE 10. ANALYSIS OF HOT-PRESSED BILLETS

Material	Billet	Amount of Indicated Element Found in Billet, w/o									
		Hf	Zr	Ta	W	Nb	Mo	C	C_{free}	N_2	O_2
HfN-10 w/o W	A	83.5	--	--	10.20	--	--	--	--	4.25	0.0320
	B	82.4	--	--	9.70	--	--	--	--	2.66	0.0025 0.0490 (a)
HfN-10 w/o TaN-10 w/o W	A	77.0	--	9.48	9.55	--	--	--	--	2.90	0.0130
	B	77.3	--	9.60	9.52	--	--	--	--	5.94	0.0098
HfC-10 w/o W	A	85.1	--	--	9.67	--	--	5.48	<.01	--	0.0440
	B	85.0	--	--	9.58	--	--	5.42	<.01	--	0.0500
HfC-10 w/o TaC-10 w/o W	A	74.7	--	9.20	10.00	--	--	5.88	<.01	--	0.0330
	B	74.0	--	9.33	10.20	--	--	5.93	<.01	--	0.0470
HfC-8 w/o Mo-2 w/o NbC	A	83.5	--	--	--	1.82	8.37	6.27	<.01	--	0.0470
	B	84.4	--	--	--	1.82	8.47	6.30	<.01	--	0.0270
ZrC-17 w/o W	A	--	81.7	--	9.79	--	--	8.30	<.01	--	0.1300
	B	--	81.9	--	9.75 (b) 16.5	--	--	8.24	<.01	--	0.0650

(a) Reanalyzed.

(b) Reanalyzed by National Spectrographic.

Spectrographic analyses of the hot-pressed billets for trace impurities are listed in Table 11. No significant increase in impurities over those listed for the starting materials are indicated other than those normally encountered in ball milling and crushing.

Lattice parameters for the hot-pressed billets are reported in Table 12. Values measured for hafnium nitride (4.524) correspond to those for a substoichiometric material having the composition $HfN_{0.74}$ as reported in the literature (ref. 3 and ref. 4, p. 218). Hafnium carbide materials are indicated to be stoichiometric according to a reported lattice parameter of 4.643 (ref. 4, p. 92), and zirconium carbide values are slightly substoichiometric when compared to a literature value for $ZrC_{0.95}$ of 4.698 (ref. 4, p. 92).

Photomicrographs shown in Figures 3 through 14 are representative of each hot-pressed billet in the as-polished condition, to illustrate the dispersion of additives and porosity, and in the etched (50 v/o lactic acid-25 v/o nitric acid-5 v/o hydrofluoric acid-20 v/o water) condition, to illustrate grain size. Density was measured from the as-polished photomicrographs utilizing the point-count technique. This procedure involves the overlay of a sized grid on the photomicrograph and visually counting intersections of the grid coinciding with the porosity. Values of density determined by point count are compared with average bulk density and calculated theoretical density in Table 13. Grain size as measured from the representative 100X-magnification photomicrographs is also included in the table. Since no grain growth was indicated metallographically, and ball milling was conducted for an equal period of time for each powder batch (15 hr), the grain size may be interpreted as an indication of the friability of the powder.

It will be noted that the dispersions are homogeneous and uniform. However, no tungsten can be identified in the zirconium carbide samples, indicating the high solubility of tungsten in ZrC.

Scanning electron micrographs of the fractured surfaces of the bend test specimens are shown in Figures 15 through 20. The secondary emission technique was utilized. A high degree of bonding is indicated between particles in all specimens examined, with transgranular fracture predominating.

Bend tests to determine modulus of rupture were conducted on 0.125 by 0.125 by 1-in. specimens using a three-point system on an Instron testing machine. Both bend load and deflection were measured and fracture modulus was calculated considering brittle fracture. Values determined are presented in Table 14. In conducting bend tests on brittle materials it is advantageous to use a large specimen to minimize the effects of surface or internal defects on rupture strength. The good agreement of values measured on duplicate specimens indicates a high degree of homogeneity and a lack of surface flaws or internal defects.

TABLE 11. SPECTROGRAPHIC ANALYSIS OF HOT-PRESSED BILLETS

Material	Billet	Amount of Indicated Impurity Found[a], ppm									
		Si	Fe	Mg	Mn	Al	Mo	Cu	Ni	Cr	Ca
HfN-10 w/o W	A	<10	50	<5	<5	10	<10	10	15	20	<10
	B	<10	100	<5	<5	10	<10	50	30	20	10
HfN-10 w/o TaN-10 w/o W	A	<10	50	<5	<5	<10	<10	30	15	10	10
	B	<10	30	<5	<5	<10	<10	30	15	10	10
HfC-10 w/o W	A	<10	<10	<5	<5	<10	20	10	<10	<10	<10
	B	<10	<10	<5	<5	<10	20	10	<10	<10	<10
HfC-10 w/o TaC-10 w/o W	A	<10	100	<5	<5	<10	<10	10	15	20	10
	B	<10	100	<5	<5	<10	<10	10	15	20	20
HfC-8 w/o Mo-2 w/o NbC	A	<10	200	<5	<5	<10	M	150	30	20	40
	B	<10	100	<5	<5	<10	M	100	20	10	10
ZrC-17 w/o W	A	<10	100	<5	<5	10	500	<10	30	50	<10
	B	<10	100	<5	<5	10	500	<10	30	50	<10

(a) Other impurities were sought but not found. The accuracy of the determination is ± 50 percent.

TABLE 12. LATTICE PARAMETERS FOR HOT PRESSED BILLETS

Material	Billet	Lattice Parameter (A_o) $\pm$ 0.001
HfN-10 w/o W	A B	4.523 4.526
HfN-10 w/o TaN-10 w/o W	A B	4.525 4.523
HfC-10 w/o W	A B	4.646 4.641
HfC-10 w/o TaC-10 w/o W	A B	4.643 4.644
HfC-8 w/o Mo-2 w/o NbC	A B	4.623 4.623
ZrC-17 w/o W	A B	4.678 4.678

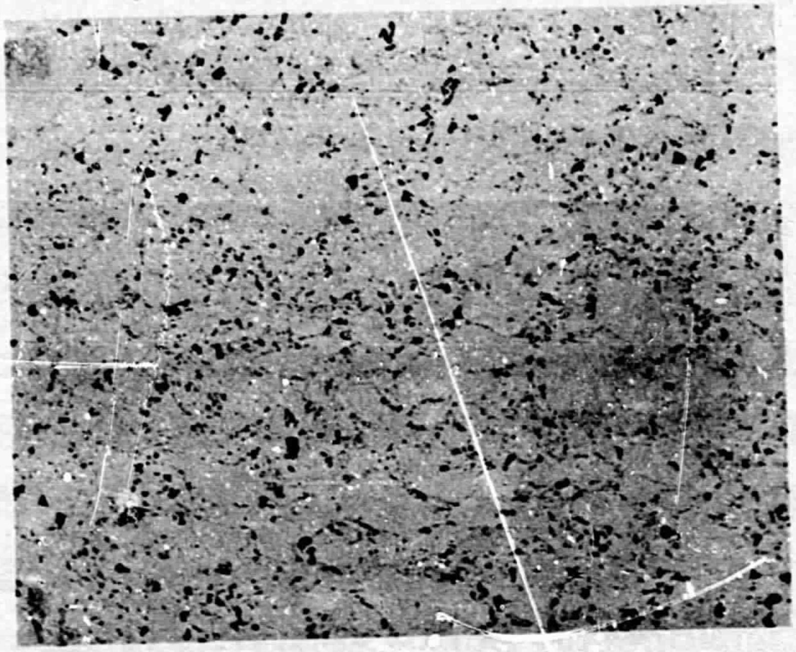

100X 2F093

a. As Polished

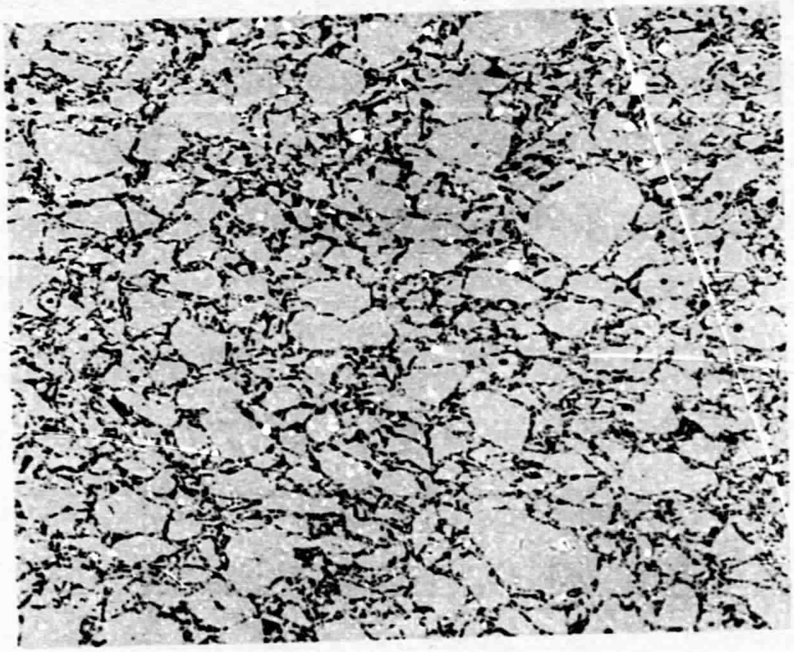

100X 2F094

b. Etched

FIGURE 3. MICROSTRUCTURE OF HfN-10 w/o TUNGSTEN BILLET A

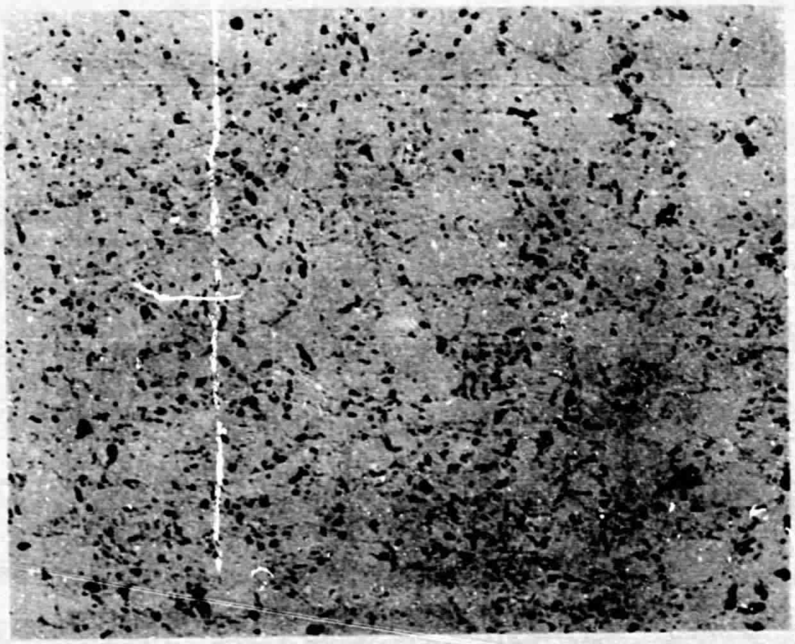

100X 2F097

a. As Polished

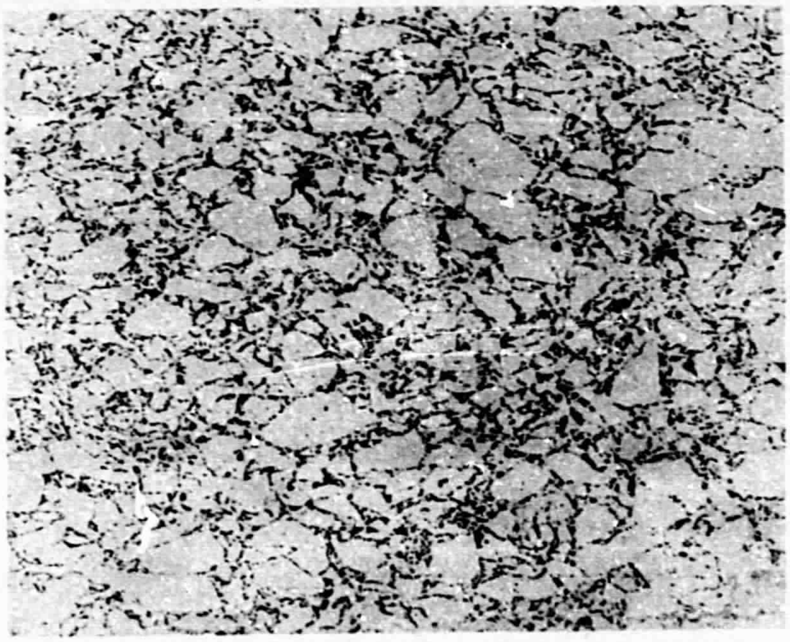

100X 2F098

b. Etched

FIGURE 4. MICROSTRUCTURE OF HfN-10 w/o TUNGSTEN BILLET B

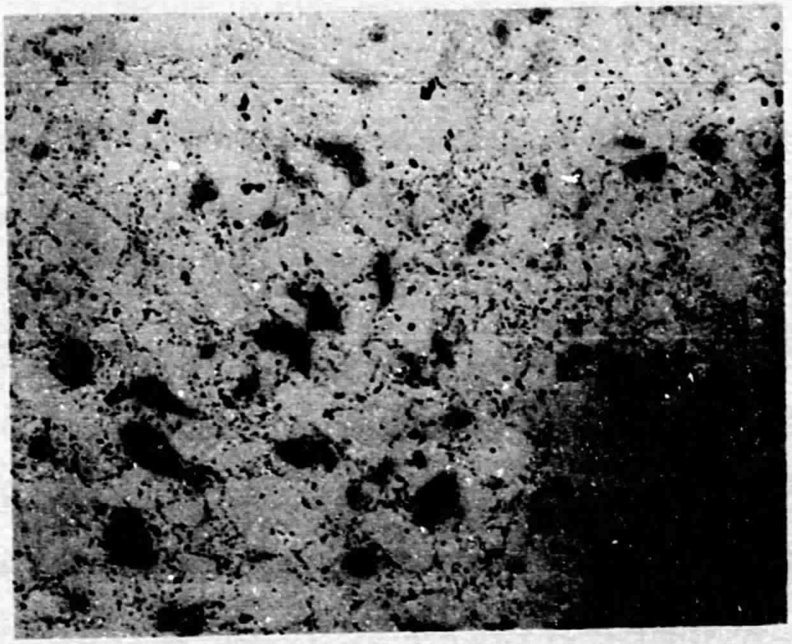

100X 2F101

a. As Polished

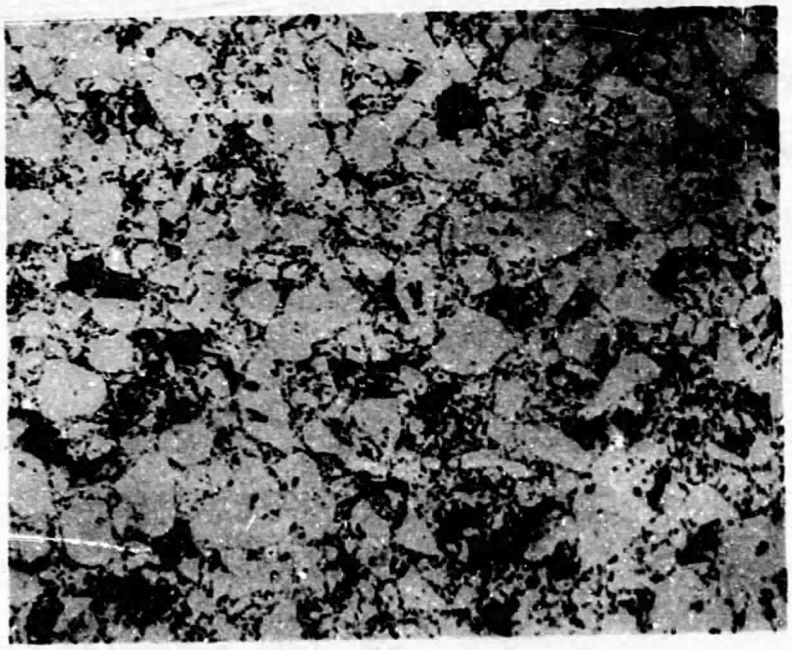

100X 2F102

b. Etched

FIGURE 5. MICROSTRUCTURE OF HfN-10 w/o TaN-10 w/o TUNGSTEN BILLET A

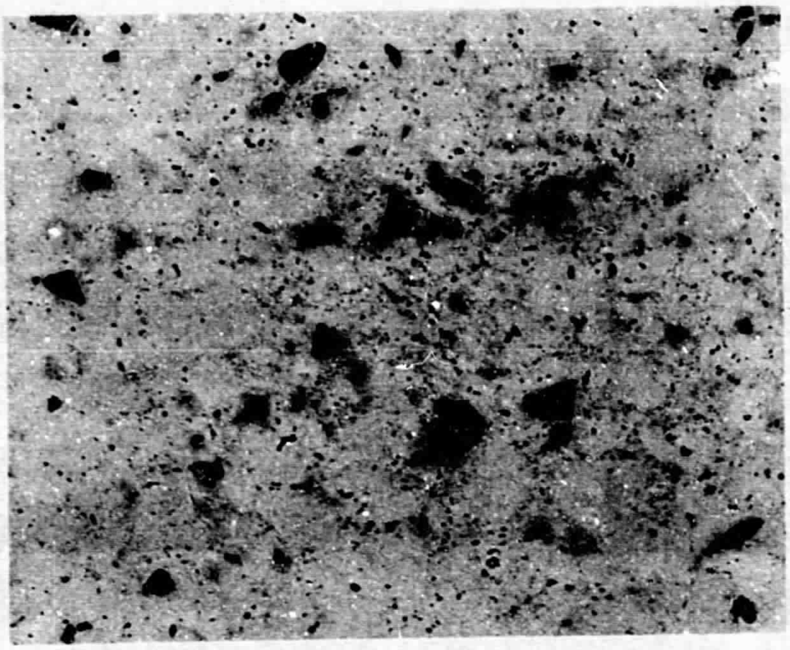

100X 2F105

a. As Polished

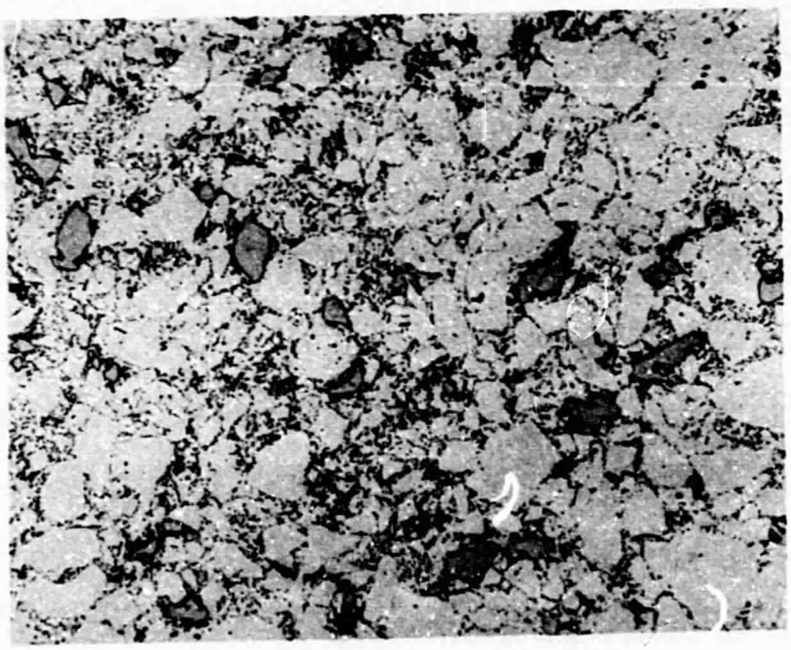

100X 2F106

b. Etched

FIGURE 6. MICROSTRUCTURE OF HfN-10 w/o TaN-10 w/o TUNGSTEN BILLET B

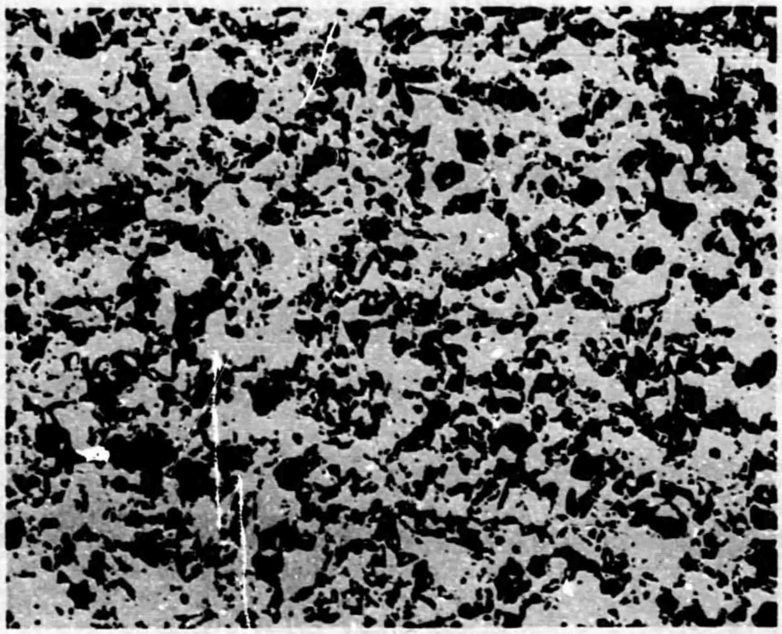

100X 2F429

a. As Polished

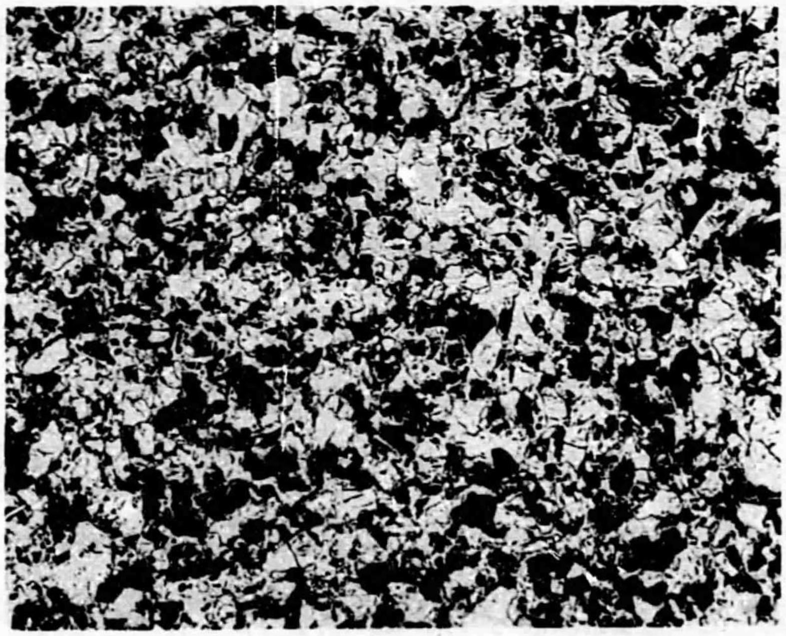

100X 2F433

b. Etched

FIGURE 7. MICROSTRUCTURE OF HfC-10 w/o TUNGSTEN BILLET A

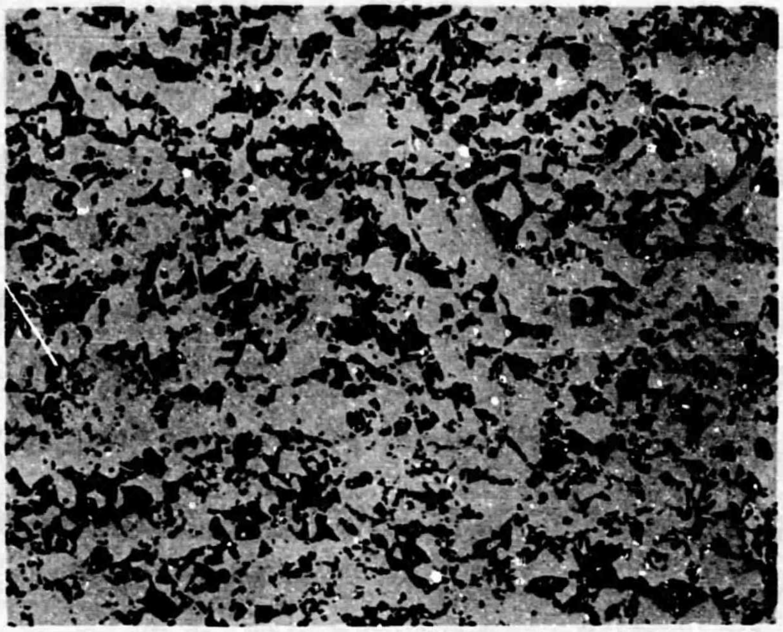

100X 2F431

a. As Polished

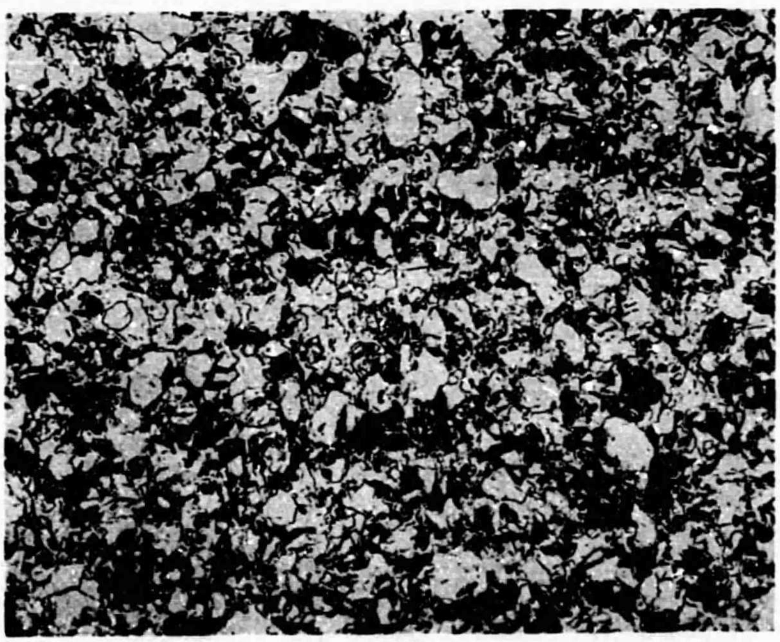

100X 2F435

b. Etched

FIGURE 8. MICROSTRUCTURE OF HfC-10 w/o TUNGSTEN BILLET B

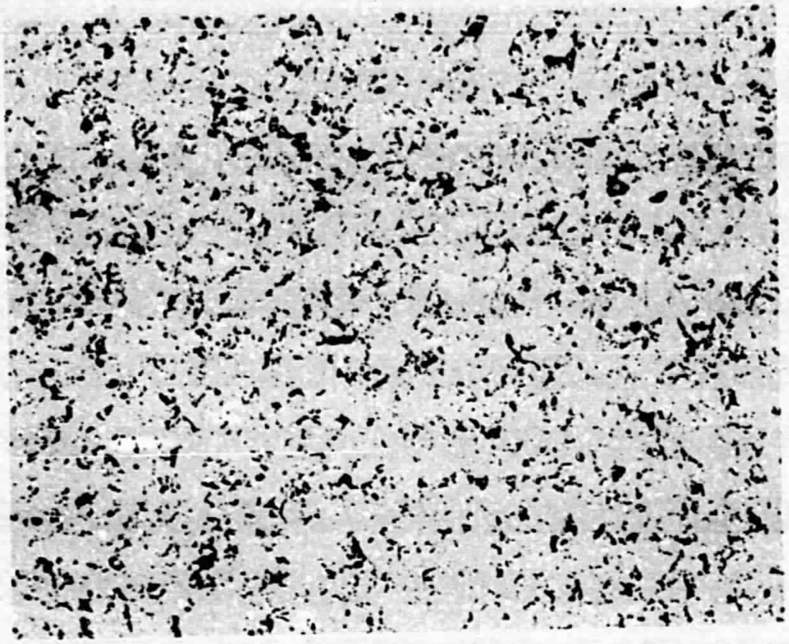

100X 2F150

a. As Polished

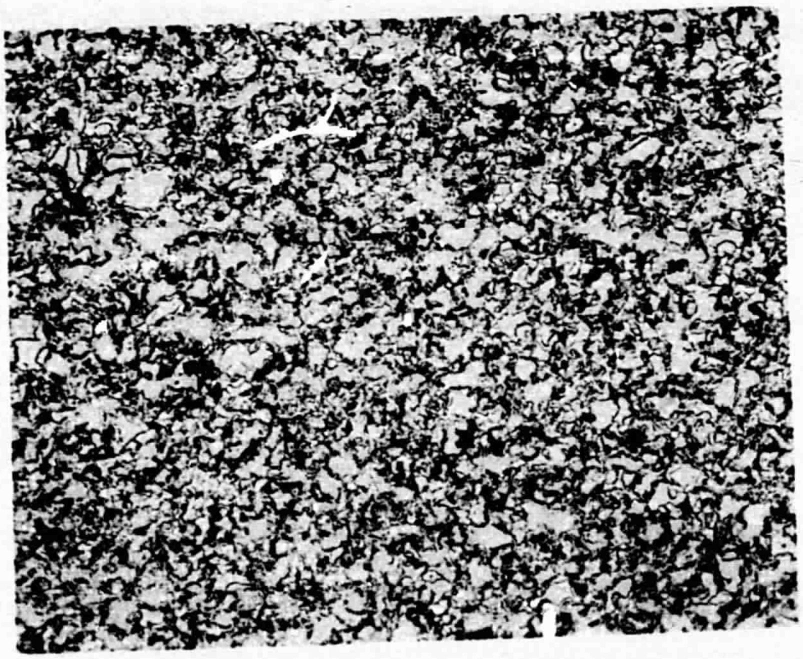

100X 2F158

b. Etched

FIGURE 9. MICROSTRUCTURE OF HfC-10 w/o TaC-10 w/o TUNGSTEN BILLET A

100X 2F152

a. As Polished

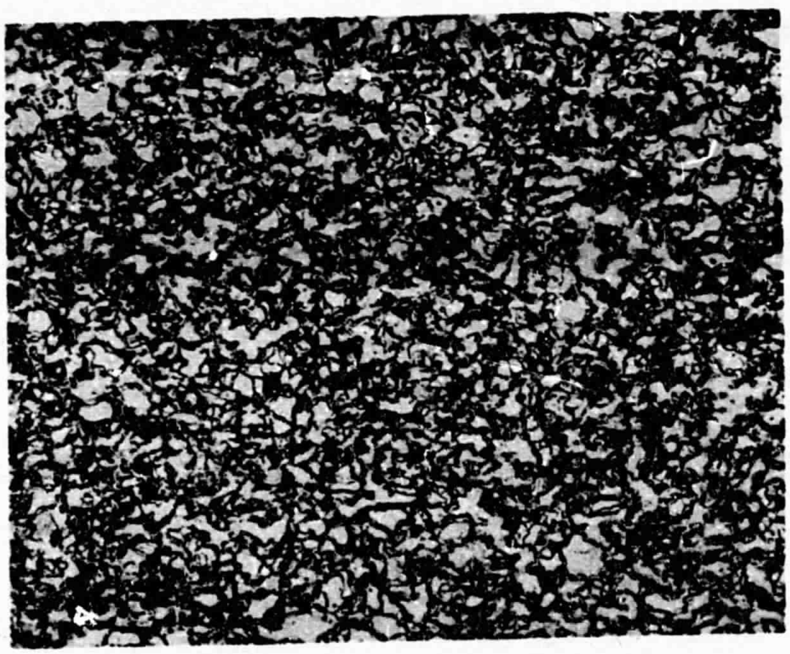

100X 2F160

b. Etched

FIGURE 10. MICROSTRUCTURE OF HfC-10 w/o TaC-10 w/o TUNGSTEN BILLET B

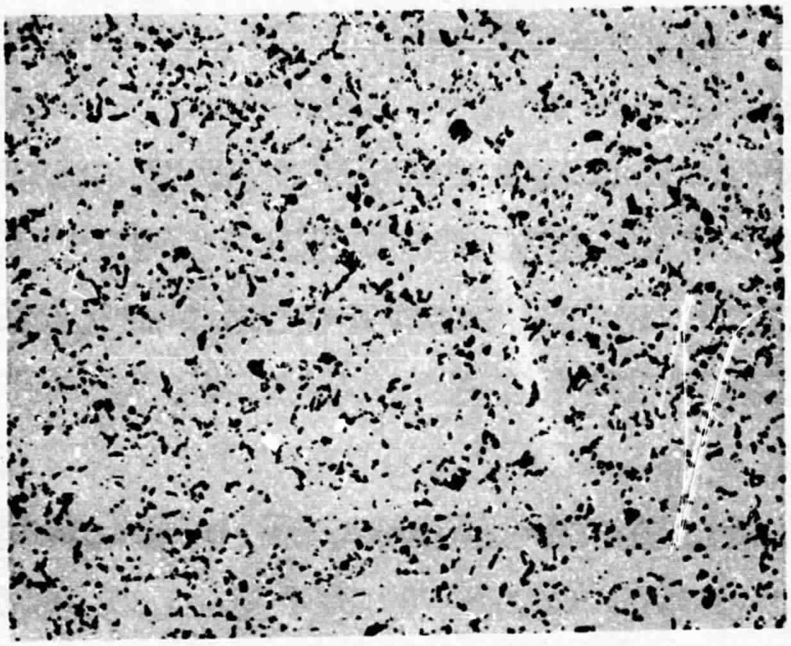

100X 2F154

a. As Polished

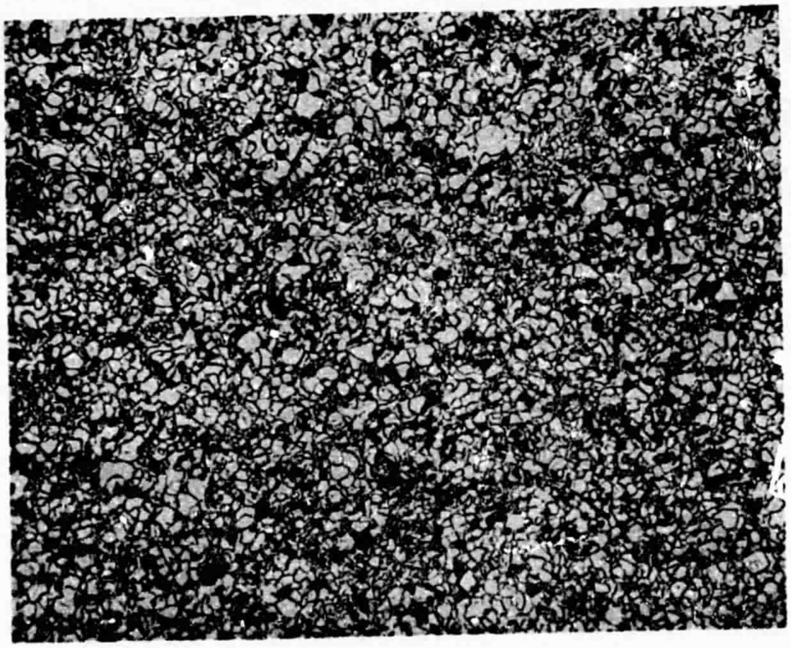

100X 2F162

b. Etched

FIGURE 11. MICROSTRUCTURE OF HfC-8 w/o MOLYBDENUM-2 w/o NbC BILLET A

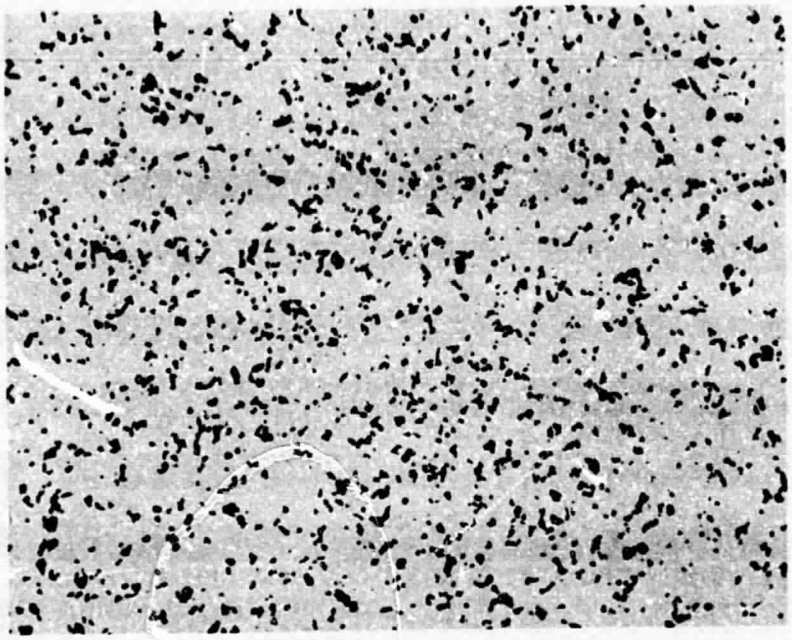

100X 2F156

a. As Polished

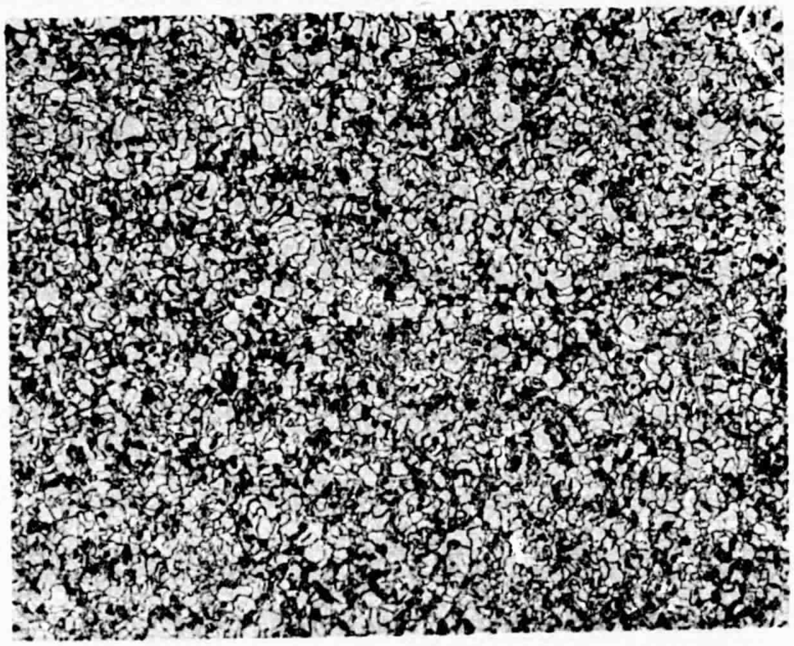

100X 2F164

b. Etched

FIGURE 12. MICROSTRUCTURE OF HfC-8 w/o MOLYBDENUM-2 w/o NbC BILLET B

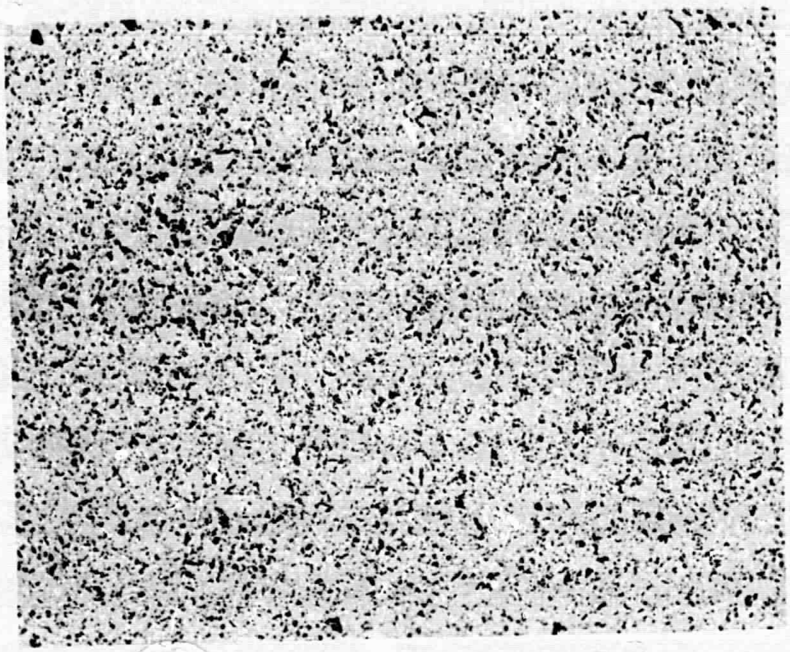

100X 2F421

a. As Polished

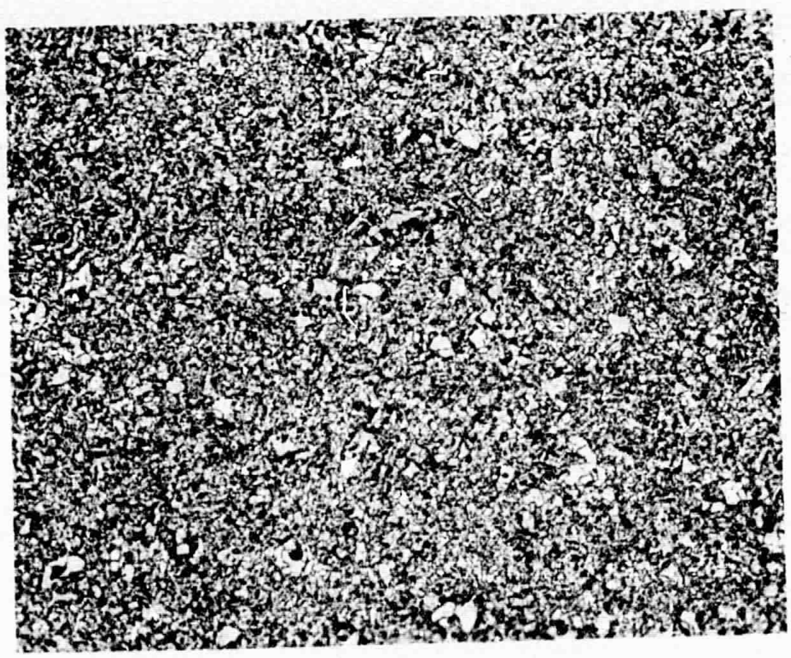

100X 2F425

b. Etched

FIGURE 13. MICROSTRUCTURE OF ZrC-17 w/o TUNGSTEN BILLET A

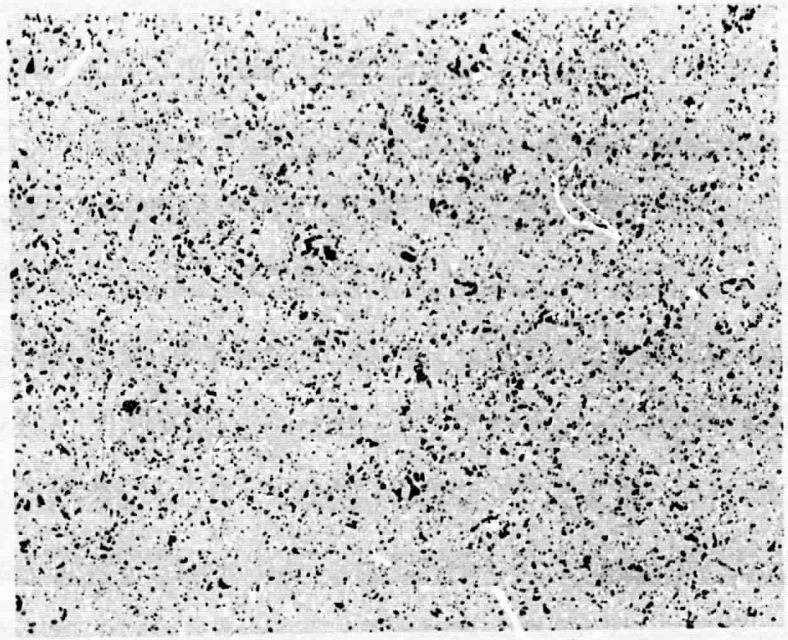

100X 2F423

a. As Polished

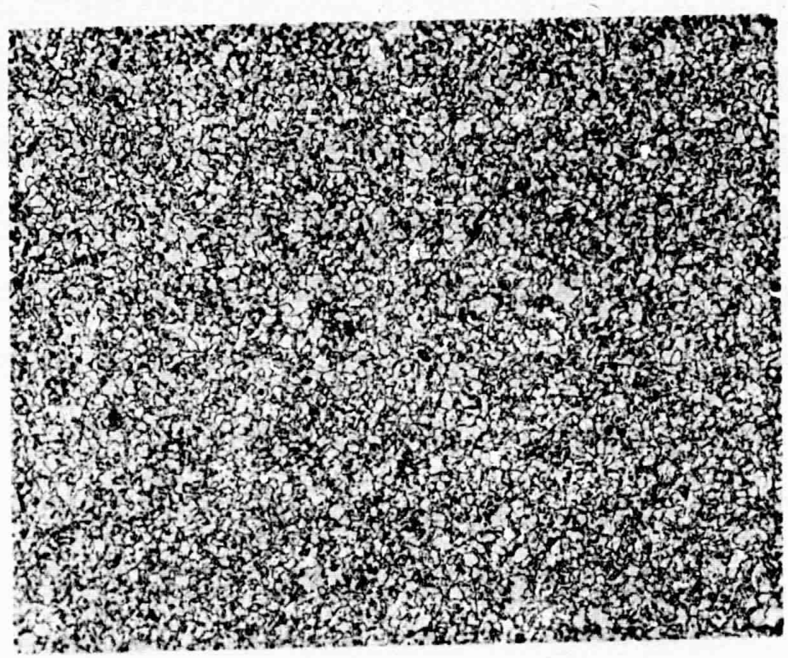

100X 2F427

b. Etched

FIGURE 14. MICROSTRUCTURE OF ZrC-17 w/o TUNGSTEN BILLET B

TABLE 13. DENSITY OF HOT-PRESSED BILLETS

Material	Billet	Theoretical Density[a], g per cm³	Average Bulk Density[b] g per cm	Average Bulk Density[b] Percent of Theoretical	Metallographic Density[c], Percent of Theoretical	Maximum Grain Size, mils
HfN-10 w/o W	A	14.210	13.38	94.1	97.9	0.7
	B	-	13.41	94.3	98.2	0.8
HfN-10 w/o TaN-10 w/o W	A	14.249	13.85	96.9	99.3	0.7
	B	-	13.85	96.9	99.4	0.7
HfC-10 w/o W	A	13.025	10.44	80.1	65.0	0.5
	B	-	10.76	82.6	72.5	0.5
HfC-10 w/o TaC-10 w/o W	A	13.231	11.86	89.8	91.3	0.4
	B	-	11.86	89.7	89.3	0.3
HfC-8 w/o Mo-2 w/o NbC	A	12.223	11.10	90.8	91.2	0.3
	B	-	11.16	91.3	91.0	0.2
ZrC-17 w/o W	A	7.420	7.32	98.7	87.1	0.2
	B	-	7.36	99.1	91.6	0.2

(a) Calculated for the nominal composition.
(b) Calculated from specimen weight and measurements.
(c) Measured by point-count technique.

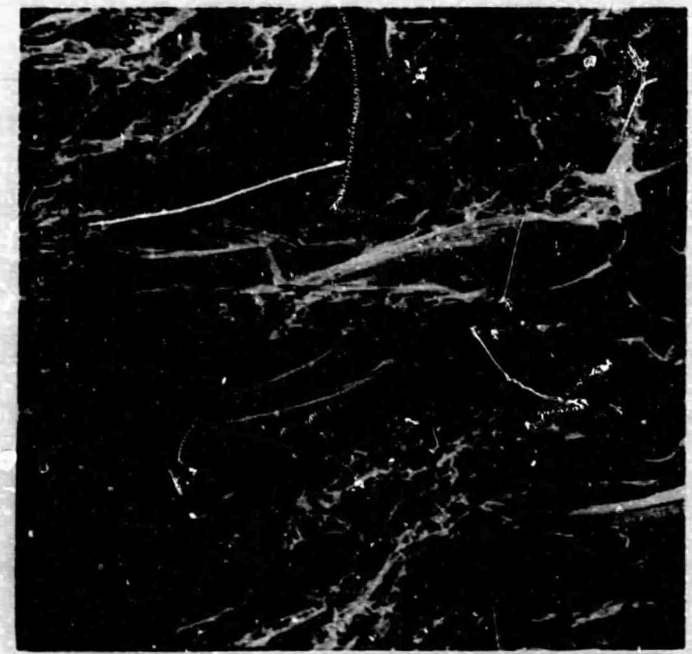

500X S4337

FIGURE 15. ELECTRON FRACTOGRAPH OF HfN-10 w/o TUNGSTEN SPECIMEN

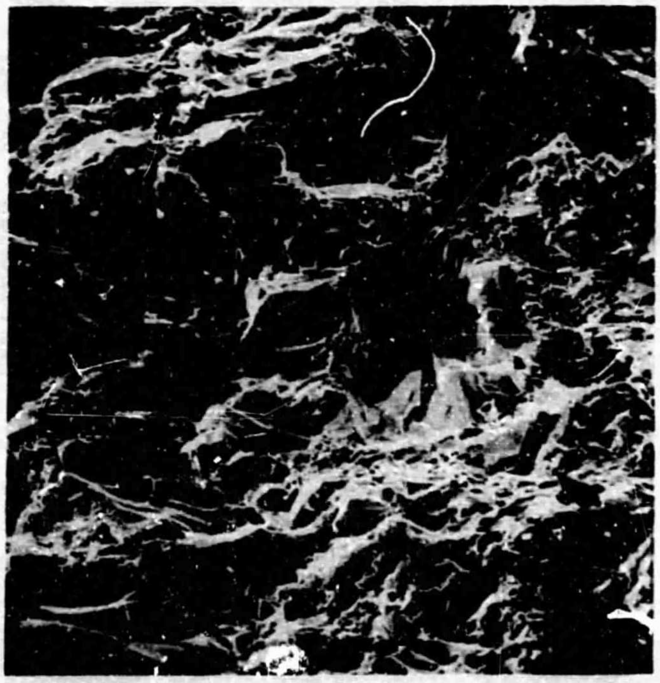

500X S4343

FIGURE 16. ELECTRON FRACTOGRAPH OF HfN-10 w/o TaC-10 w/o TUNGSTEN SPECIMEN

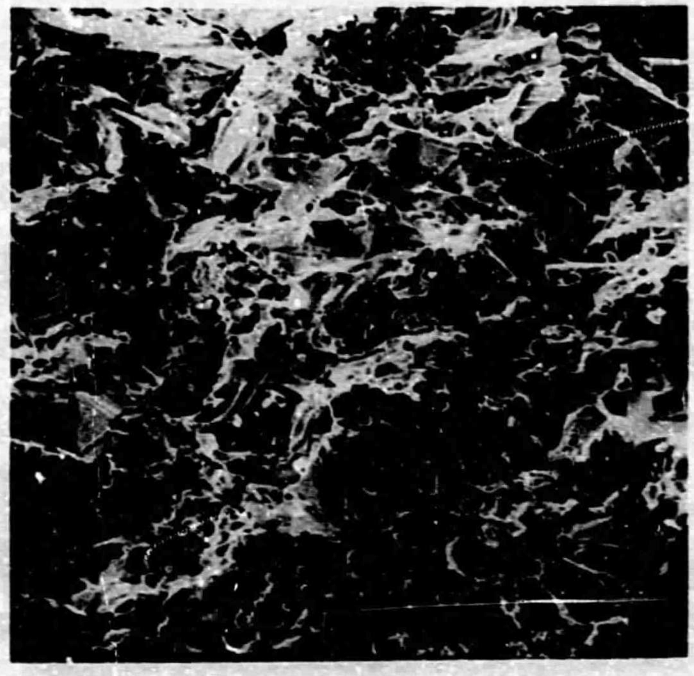

500X S4346

FIGURE 17. ELECTRON FRACTOGRAPH OF HfC-10 w/o TUNGSTEN SPECIMEN

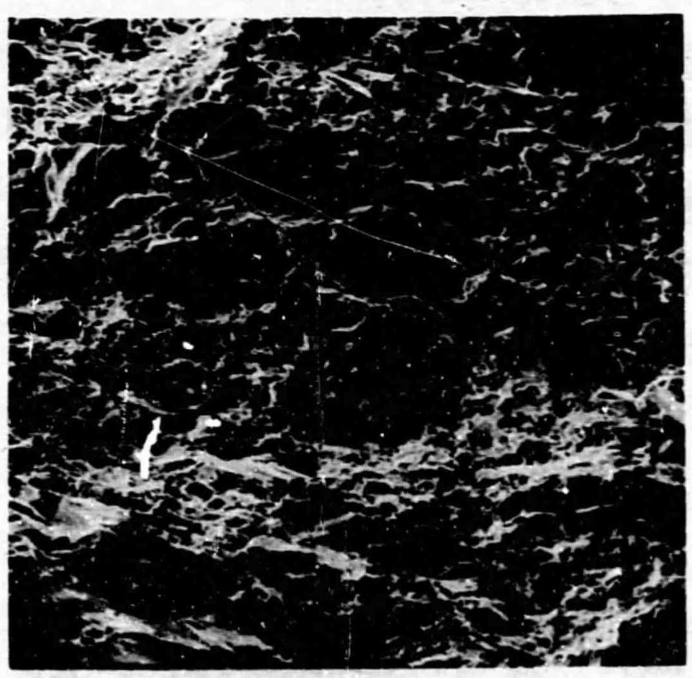

500X S4347

FIGURE 18. ELECTRON FRACTOGRAPH OF HfC-10 w/o TaC-10 w/o TUNGSTEN SPECIMEN

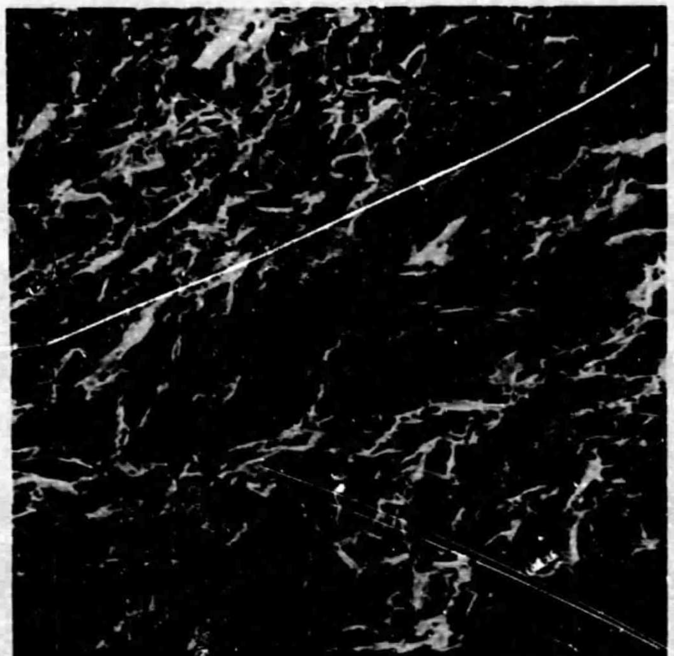

500X S4350

FIGURE 19. ELECTRON FRACTOGRAPH OF HfC-8 w/o MOLYBDENUM-2 w/o NbC SPECIMEN

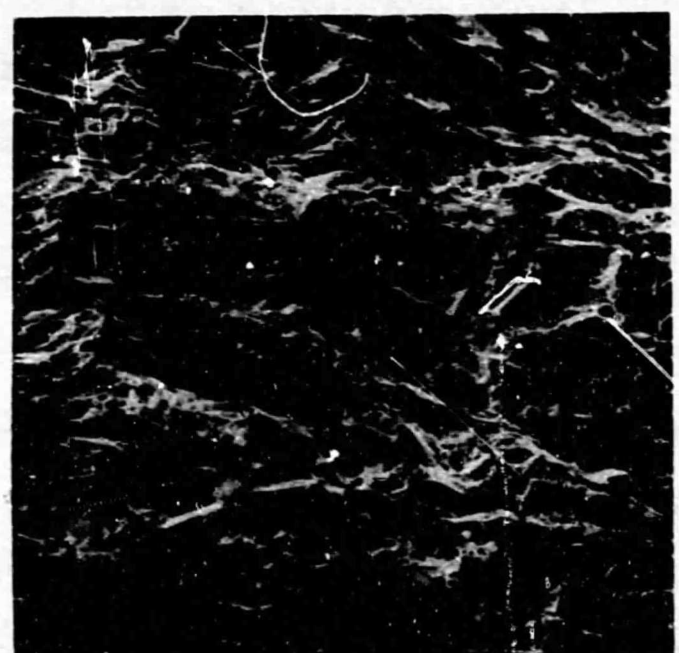

500X S4351

FIGURE 20. ELECTRON FRACTOGRAPH OF ZrC-17 w/o TUNGSTEN SPECIMEN

TABLE 14. BEND TEST DATA

Material	Billet	Load, psi	Deflection, in.	Dimensions (L = 0.750), in. b	h	Stress, psi
HfN-10 w/o W	A	63	0.0020	0.1259	0.1246	70,875
	A	65.5	0.0021	0.1259	0.1256	73,675
	B	63	0.0021	0.1257	0.1260	71,010
	B	57.5	0.0020	0.1255	0.1258	65,425
HfN-10 w/o TaN-10 w/o W	A	68	0.0016	0.1253	0.1257	77,270
	A	76	0.0015	0.1257	0.1254	86,495
	B	68	0.0016	0.1257	0.1257	77,040
	B	47	0.0014	0.1256	0.1251	53,790
HfC-10 w/o W	A	32	0.0018	0.1254	0.1254	36,510
	A	32	0.0014	0.1254	0.1254	36,510
	B	30	0.0015	0.1254	0.1251	34,385
	B	32.5	0.0017	0.1253	0.1248	37,480
HfC-10 w/o TaC-10 w/o W	A	72	0.0033	0.1259	0.1253	81,940
	A	67	0.0022	0.1257	0.1254	76,250
	B	72.5	0.0025	0.1259	0.1253	82,510
	B	76	0.0028	0.1259	0.1253	86,495
HfC-8 w/o Mo-2 w/o NbC	A	87	0.0030	0.1253	0.1262	98,070
	A	90.5	0.0027	0.1263	0.1262	101,205
	B	72.5	0.0022	0.1262	0.1261	81,280
	B	77.5	0.0024	0.1264	0.1235	90,440
ZrC-17 w/o W	A	76	0.0018	0.1247	0.1248	88,055
	A	93	0.0020	0.1249	0.1248	107,580
	B	85	0.0017	0.1248	0.1248	98,330
	B	76	0.0017	0.1249	0.1249	87,830

CONCLUSIONS

Ten corrosion test specimens of each of the required six cermet compositions were prepared and characterized. In order to fabricate the specimens it was necessary to develop processes for the synthesis of high-purity hafnium nitride and hafnium carbide powders in kilogram quantities from hafnium crystal bar. In the experiments conducted to find a suitable process it was found that the hydride-dehydride technique was suitable for preparation of hafnium powder; however, a double nitriding treatment at 1800 C was required to synthesize single-phase hafnium nitride, and a modified reactive hot-pressing technique followed by a high-temperature vacuum homogenization was required to synthesize the hafnium carbide. It was demonstrated that the high purity of the powders could be maintained throughout hot pressing by conducting all processing steps in inert-atmosphere glove boxes or vacuum-purged hot presses. The degree of purity is significant when it is considered that complete processing requires many steps, with a minimum of 20 hr at temperatures between 750 and 860 C and 32 hr at temperatures of 1800 C or above.

Blending studies and the resultant hot-pressed samples demonstrated that a sufficient volume percentage of refractory metal was not present in any of the compositions to give a continuous metal matrix. It is estimated that a minimum of 20 v/o would be required in order to achieve this requirement.

In the case of the zirconium carbide-tungsten cermet it would be necessary to experimentally determine the volume of refractory metal required, since tungsten exhibits a high solubility in zirconium carbide.

Difficulties were encountered in achieving high density in the hafnium carbide-base cermets as a result of strength limitations of the graphite punches and die bodies. Although the best commercially available high temperature-high strength graphites were used, excessive creep and failure of the dies occurred during several pressings. As expected, it was noted that the density increased in the hafnium carbide cermets when the hafnium carbide content was reduced, as in the case of the HfC-TaC-tungsten composition or when molybdenum was substituted for tungsten.

Analytical difficulties were encountered when attempts were made to determine the oxygen content of the cermets using vacuum-fusion analysis. Inert-gas fusion was used for reanalysis of several samples and for the final characterization of the specimens. Although inert-gas fusion is considered to be more accurate, additional analytical specimens would be appropriate for complete characterization of the billets in respect to oxygen.

Metallographic examination of the cermets indicated a high degree of bonding and a homogeneous distribution of the refractory-metal and cermet additives. The degree of homogeneity and the lack of defects were confirmed by the uniformity of the modulus-of-rupture results for each composition.

REFERENCES

(1) Waldo, C. T., and Anderson, W. K., "Crystal Bar Hafnium Powder, Its Production, Mechanical and Corrosion Properties", KAPL-M-CTW-2 (1957).

(2) Edwards, R. K., and Malloy, G. T., "The Rate of Reaction of Nitrogen With Hafnium Metal", USAEC File No. NP-6212 (1956).

(3) Booker, P. N., and Brukl, C. E., "The Phase Equilibria in the Metal Rich Region of the Hafnium-Tantalum-Nitrogen System", AFML-TR-69-117, Part VI (1969).

(4) Goldschmidt, H. J., Interstitial Alloys, Plenum Press, New York (1967).